In Vivo Structural Analysis of Subchondral Trabecular Bone in Osteoarthritis of the Hip using Multi-Detector Row CT

KO CHIBA[1] M.D., MASAKO ITO[2] Ph.D., M.D., MAKOTO OSAKI[1] Ph.D., M.D., MASATAKA UETANI[2] Ph.D., M.D., HIROYUKI SHINDO[1] Ph.D., M.D.

[1]Department of Orthopaedic Surgery, Nagasaki University School of Medicine, Japan
[2]Department of Radiology, Nagasaki University School of Medicine, Japan

Abstract

Objective: With developments in clinical CT, in vivo analysis of patients' bone microstructure has become increasingly possible. The subchondral trabecular bone of hip osteoarthritis (OA) patients using multi-detector row CT (MDCT) was analyzed to closely examine the structural changes that occur as OA progresses.

Design: 47 female hip joints were studied: 20 with OA secondary to hip dysplasia (11 advanced OA, 9 early-moderate OA), 7 with hip dysplasia without OA, and 20 normal. The images' maximal spatial resolution was $280\times280\times500$ μm. Regions of interest were the subchondral trabecular bones of the acetabulum and femoral head. Measurement parameters were bone volume fraction (BV/TV), trabecular thickness (Tb.Th), trabecular number (Tb.N), trabecular separation (Tb.Sp), structure model index (SMI), trabecular bone pattern factor (TBPf), Euler's number, and trabecular anisotropy (DA). Relationships between joint space volume and these parameters were analyzed.

Results: With decreasing joint space, Tb.Th and BV/TV increased, and Tb.Sp, Tb.N, SMI, TBPf, and DA decreased significantly. The microstructures were significantly different between the early to advanced OA groups and the normal and dysplasia groups; there was no significant difference between the normal and dysplasia groups.

Conclusions: Changes of subchondral trabecular bone structure in OA could be evaluated using MDCT, despite imperfect spatial resolution and limited accuracy. Trabecular bone thickening and associated structural changes may be closely related to OA. Changes were observed in early to advanced OA, but not in dysplasia. This method may help further elucidate OA pathogenesis, determine the therapeutic strategy, and evaluate therapy.

Key Words: osteoarthritis of the hip, subchondral trabecular bone, microstructure, computed tomography (CT)

Introduction

Osteoarthritis (OA) is a disease characterized by cartilage attrition and joint pain. The importance of subchondral bone in the etiology of OA has long been understood. The subchondral bone of OA exhibits various changes, such as trabecular bone thickening, cyst formation, decreased bone mineralization, and increased bone turn-over[1]. Trabecular bone thickening leads to bone sclerosis, which in turn causes decreased shock absorbency and cartilage damage[2]. High bone turn-over increases the release of various cytokines from subchondral bone, which can lead to cartilage degeneration. In OA animal models, subchondral bone resorption increases in the early stage. By using bone resorption inhibitor drugs, prevention of cartilage attrition has been reported[3]. In other words, subchondral bone and cartilage influence each other strongly, and subchondral bone changes in OA are not only the result of cartilage attrition, but the cause of cartilage attrition.

The cartilage has no nerve supply, and the main cause of pain in OA is thought to be bone pain. The bone marrow lesion seen in OA subchondral bone on MRI is associated with microfractures, and a strong relationship with OA pain has been reported[4].

Disease-modifying OA drugs (DMOADs) are drugs aimed at fundamental treatment of OA; they are expected to become a mainstay of treatment for OA in the future. The target tissue includes the subchondral bone, in addition to the articular cartilage and synovium. In other words, by early detection of OA and by normalization of bone metabolism and bone structure, OA progression and symptoms may be preventable. Candidate drugs currently reported include alendronate, risedronate, and calcitonin[3,5,6]. Osteotomy also improves OA progression and symptoms by altering the mechanical environment of the joint. After the surgery, normalization of trabecular structure, such as decreased bone sclerosis and a reduction in bone cysts, has been observed.

Therefore, evaluation of subchondral bone, in addition to cartilage, by clinical imaging techniques is very important in analyzing the etiology of OA and assessing treatment in patients.

Generally, analysis of bone microstructure has been performed by pathological examination or micro CT, which basically provides in vitro analysis only for the extracted bone samples. However, owing to the remarkable development of clinical medical imaging such as CT and MRI in recent years, it is possible to analyze patients' bone microstructure in vivo. Multi-detector row computed tomography (MDCT), which has become widespread and is able to scan thin slice images in a short time, provides higher resolution images than before. Several studies have shown the usefulness of in vivo bone microstructure analysis by MDCT in osteoporosis cases[7,8].

In this study, a cross-sectional analysis of the subchondral trabecular bone microstructure of

patients with hip OA using clinical MDCT was conducted to answer the following research questions: whether changes in trabecular bone structure in hip OA can be evaluated with clinical CT; what kinds of changes are most pronounced; and when and where those changes occur.

Methods

Subjects

Twenty female patients with hip OA secondary to hip dysplasia and 20 female normal volunteers were investigated from 2007 to 2008. The hip OA patients had undergone CT examination for hip OA surgery. Patients with hip OA secondary to avascular necrosis, rheumatoid arthritis, or trauma and those with a history of osteotomy or contralateral arthroplasty were excluded. The normal volunteers had undergone health checks at our hospital and volunteered to participate in this study. They were interviewed and underwent CT examinations, after which those who had hip joint disease or were taking medications that could affect bone metabolism were excluded. The analysis included 47 hip joints: 11 hip joints were advanced OA (Tönnis grade 3), 9 were early to moderate OA (grade 1-2), 7 were hip dysplasia without OA, and 20 were normal hips[9]. Hip joints on the unaffected side in OA patients were excluded from the analysis. In the normal volunteers, only the left hip was analyzed.

The mean age was 69 ± 6 (range 59-81) years for advanced OA, 66 ± 10 (45-81) years for early-moderate OA, 63 ± 9 (49-74) years for hip dysplasia without OA, and 66 ± 9 (50-80) years for normal volunteers (p=0.412). The center-edge (CE) angle was 19 ± 12 (2-43)° in the advanced group, 12 ± 13 (-17-28)° in the early-moderate group, 12 ± 8 (0-20)° in the dysplasia group, and 36 ± 5 (27-44)° in the normal group. The CE angle is formed by a line from the center of the femoral head to the lateral edge of the acetabular roof and a vertical line drawn through the center of the femoral head[10]. The acetabular angle was 43 ± 4 (34-50)° in the advanced group, 43 ± 4 (38-48)° in the early-moderate group, 47 ± 4 (43-55)° in the dysplasia group, and 39 ± 2 (35-43)° in the normal group. The acetabular angle is formed by a horizontal line connecting both tear drops and a line from a tear drop to the lateral edge of the acetabular roof[11]. The study protocol was approved by the ethics review board of our institute and complied with the Declaration of Helsinki of 1975, revised in 2000.

CT scanning

An MDCT with 16 detectors (Aquilion 16, Toshiba, Tokyo, Japan) was used. Scanning was performed at 120 kV, 300 mAs, and 0.5-mm thickness. Images were reconstructed with a field of view (FOV) of 70 mm, 512×512 pixel matrix, and 0.2-mm pitch (Fig. 1). The maximal

in-plane resolution was 280×280 μm^2, and the axial resolution was 500 μm, based on the manufacturer's data. CTDIvol was 19.7 mGy, and DLP was 331 mGy, which were almost the same as for conventional abdominal CT scans.

Microstructure Analysis

The microstructure of subchondral trabecular bone was measured by bone structure measurement software (TRI/3D-BON, Ratoc System Engineering Co., Tokyo, Japan). CT images were reconstructed to coronal images for bone structure analysis to facilitate differentiation between cartilage and subchondral bone. Regions of interest (ROIs) were subchondral trabecular bones of the acetabulum and femoral head, 1 cm under the subchondral endplate, 2×2 cm^2 area, and aligned with the principal compressive trabeculae of the femoral head (Fig. 2). The bone cyst region was strictly excluded from the ROIs. The joint space volume aligned with the ROI was also measured. ROI was established semi-automatically by a single orthopedist. Square columns of 2×2 cm^2 were set manually, and cartilage was manually corrected after being automatically extracted. Using the magnification function, a region 1 cm from the subchondral endplate was specified. The binarization was performed using a fixed threshold value, which was calculated by a discriminant analysis between the bone and the background in the histogram. Threshold values were obtained from 8 normal volunteers' femoral head trabecular bone areas, and their mean was defined as the fixed threshold value.

The measurement parameters were apparent bone volume fraction (app BV/TV), apparent trabecular thickness (app Tb.Th), apparent trabecular number (app Tb.N), apparent trabecular separation (app Tb.Sp), structure model index (SMI), trabecular bone pattern factor (TBPf), Euler's number, and degree of anisotropy (DA)[12-15]. SMI is an index evaluating whether trabecular bone is rod-like or plate-like, and a small value means a more plate-like structure. TBPf is also an index evaluating rod-like, plate-like, or honeycomb-like structure, and a small value means a more honeycomb-like structure. Euler's number represents the connectivity of trabecular bone, and a small value means a more connected structure. In trabecular bone converted to a linear drawing, this was defined as Euler number = number of trabecular bone components – number of through holes + number of cavities. Connectivity is higher when there is a greater number of through holes. DA was determined from the ratio between the maximal and minimal radii of the mean intercept length (MIL) ellipsoid. The mean length of lines cut by lines parallel to an arbitrary angle is called the MIL. When plotted on polar coordinates, this resembles an ellipsoid, which is called an MIL ellipsoid. By taking the ratio of the long and short axes of the ellipsoid, anisotropy can be quantified.

The reproducibility of the measurements was estimated by calculating the intra-class

correlation coefficient (ICC) of 3 investigators' measurements of 3 randomly chosen CT studies 3 times. Intra-tester reproducibility and inter-tester reproducibility were: 0.64 and 0.66, respectively, for BV/TV; 0.97 and 0.97, respectively, for Tb.Th; 0.99 and 0.99, respectively, for Tb.N; 0.98 and 0.97, respectively, for Tb.Sp; 0.99 and 0.99, respectively, for SMI; 0.97 and 0.97, respectively, for TBPf; 0.99 and 0.99, respectively, for Euler's number; and 0.99 and 0.99, respectively, for DA.

Statistical Analysis

The relationships between joint space volume, CE angle, acetabular angle, and these microstructure parameters were analyzed by Pearson's correlation test. Differences in these microstructure parameters among the normal, dysplasia, early-moderate OA, and advanced OA groups were analyzed using the Bonferroni test (SPSS 16.0, Chicago, IL, USA). $P<0.05$ was considered statistically significant.

Results

As the joint space narrowed, trabecular bone thickened, bone volume fraction increased, and the trabecular morphology became more plate-like and honeycomb-like on both the acetabular and femoral head sides. In addition, on the acetabular side, the distance between bone trabeculae lessened, and anisotropy decreased as the joint space narrowed. On the femoral head side, there were fewer bone trabeculae and decreased connectivity as the joint space narrowed (Table 1). The same tendencies were also seen in the relation between the CE angle and trabecular bone structure, but the correlation coefficient with the acetabular angle was small (Table 2).

These changes were significant from early-moderate OA on the acetabular side, and they occurred prominently in advanced OA (Table 3). On the femoral head side, changes in number, though not significant, appeared in early-moderate OA. Then, in advanced OA, they were significant (Table 4).

Figure 3 is the scattergram of the joint space volume and app trabecular thickness of the femoral head subchondral bone. They had a negative correlation ($r=-0.665$, $p<0.001$), and the app trabecular thickness increased in early to advanced OA, but not in dysplasia. Figure 4 shows the 3D reconstructed MDCT images of subchondral trabecular bone of normal and advanced OA cases. The subchondral trabecular bone of the advanced OA patient shows thickening and union of trabecular bones.

Discussion

To the best of our knowledge, there has been no previously reported in vivo analysis of the subchondral bone microstructure of patients with hip dysplasia and OA using clinical MDCT. So far, in vivo analysis of human trabecular bone by clinical MDCT has been performed mainly for the evaluation of osteoporosis. Ito et al. evaluated vertebral microstructure and fracture risk using MDCT, showing superior predictive ability than dual x-ray absorptiometry[7]. Graeff et al. also studied vertebral microstructure by MDCT and monitored drug-associated changes[8].

In recent years, several studies have shown the possibility of in vivo analysis of human hip joints by clinical MDCT. Bauer et al. analyzed the trabecular structure of bone samples from the femoral head by MDCT in a simulated soft-tissue environment; they concluded that the major characteristics of the trabecular network could still be appreciated and quantified, even though soft tissue scatter substantially compromises image quality[16]. Diederichs et al. also showed the feasibility of measuring trabecular bone structure of the proximal femur using MDCT in a clinical setting[17].

In this study, we found that, as the joint space volume decreased, trabecular thickness and bone volume fraction increased. This is thought to be due to adaptation to increased loading on the joint or thickening as a repair mechanism when microfractures develop. Thickening of trabeculae would induce a decrease in trabecular separation at the acetabular subchondral bone. (Table 1). On the other hand, the trabecular thickness increased, but trabecular number decreased at the femoral head subchondral bone, which might mean that trabecular thickening caused a union of trabecular bones, resulting in decreased trabecular number. The union of trabecular bone was probably related to both true trabecular thickening and a partial volume effect (Table 1, Fig. 4). SMI and TBPf at both subchondral bone locations decreased as the joint space volume decreased. Thickening of trabecular bone would also cause more plate-like and honeycomb-like structures of the trabecular bones. DA at the acetabular subchondral bone decreased as the joint space volume decreased. Low bone volume fraction bone generally has high anisotropy to preserve only trabecular bone for weight bearing. Therefore, decreased joint space and the subsequent high bone volume fraction might decrease DA. Correlation coefficients were high for bone volume fraction, trabecular thickness, and TBPf, suggesting that these parameters were sensitive for the evaluation of OA.

Chappard et al. performed a detailed study of the subchondral bone microstructure of hip OA using synchrotron micro CT. They found that the OA subchondral bone had increased bone volume fraction and trabecular thickness, and decreased trabecular separation[1]. Ding et al. also investigated the features of subchondral bone of knee OA using conventional micro CT and showed increased bone volume fraction and trabecular thickness, and decreased SMI[18]. These

results are similar to ours. Therefore, although accuracy was limited, change of the subchondral trabecular bone structure in OA could be evaluated by MDCT to a certain extent.

These changes were observed in early to advanced OA, but not in dysplasia (Tables 3 and 4). Dysplasia alone might not cause subchondral bone changes, or small changes could not be detected because of the lack of spatial resolution. In the early-moderate OA group, significant changes were observed only at acetabular subchondral bone (Tables 3 and 4). The data suggest that OA changes in subchondral trabecular bone might occur predominantly at the acetabular side rather than the femoral head side.

Generally it is difficult to analyze bone microstructure of dysplasia and early OA patients by micro CT, because these bone samples are not easily available. Arthroplasty is usually performed for advanced OA patients, and it is hard to extract subchondral bone samples from the acetabular side. Furthermore, finding cadavers with dysplasia and early OA is not easy. Therefore, information regarding the bone microstructure of dysplasia and of early OA patients is valuable.

In the future, the therapeutic approach to OA will shift to early detection, prognosis prediction, and preventive therapy. This method may play a useful role in all these steps. Using this method, we could predict which OA patients would develop destructive changes, with atrophic and collapse changes. Furthermore, we could use this method to determine whether osteotomy and DMOADs were indicated, and evaluate the effects of these treatments. This study could be a first step in realizing these potential uses.

The limitation of this study was limited accuracy. The spatial resolution of this method was $500 \times 280 \times 280$ μm^3, which is basically insufficient to allow perfect visualization of trabecular bone. It causes a partial volume effect; several trabecular bones unite with each other and look like one large trabecular bone, and small trabecular bone cannot be detected and vanishes, looking like there is no bone (Fig. 1). In addition, there is more noise in clinical CT images than in experimental images because of soft tissues and patient movement[16,17]. Our group has already reported an in vivo analysis of trabecular bone microstructure using MDCT, which had a spatial resolution of $500 \times 210 \times 210$ μm^3 that was similar to that in the present study. In this report, we confirmed the validity of the accuracy of this method by comparing the MDCT images with the micro CT images[7]. Other papers also suggest the possibility of in vivo microstructure analysis of the hip joint by MDCT[16,17]. Advances in MDCT continue to be made, and the spatial resolution is increasing, with less noise and lower radiation doses. These advances will likely lead to fewer accuracy problems in the future.

This study was a cross-sectional study, and a longitudinal study might show earlier changes of OA subchondral trabecular bone. Strictly speaking, the joint space volume is not equal to the

cartilage volume. However, we think that the gap between the acetabular and femoral cartilages would be so small that such error is acceptable.

In conclusion, we have shown the possibility of evaluating trabecular structure in hip OA patients using clinical CT. Increased trabecular bone width and accompanying structural changes may be closely related to OA. These changes do not appear in the stage with dysplasia only, but they appear when the condition reaches early-moderate OA, predominantly on the acetabular side. This method may be applied to further elucidate the pathogenesis of OA, to decide the therapeutic strategy, and to evaluate the effects of treatment.

Author Contributions

KC: design, collection and analysis of data, and drafting of the article. MI: design, collection and analysis of data, revision of the article. MO, MU, and HS: design, collection of data, and revision of the article**.**

Competing interest statement

No competing interests declared.

References

(1) Chappard C, Peyrin F, Bonnassie A, Lemineur G, Brunet-Imbault B, Lespessailles E et al. Subchondral bone micro-architectural alterations in osteoarthritis: a synchrotron micro-computed tomography study. Osteoarthritis Cartilage 2006;14:215-23.

(2) Radin EL, Rose RM. Role of subchondral bone in the initiation and progression of cartilage damage. Clin Orthop Relat Res 1986;213:34-40.

(3) Hayami T, Pickarski M, Wesolowski GA, McLane J, Bone A, Destefano J et al. The role of subchondral bone remodeling in osteoarthritis: reduction of cartilage degeneration and prevention of osteophyte formation by alendronate in the rat anterior cruciate ligament transection model. Arthritis Rheum 2004;50:1193-206.

(4) Felson DT, Niu J, Guermazi A, Roemer F, Aliabadi P, Clancy M, et al. Correlation of the development of knee pain with enlarging bone marrow lesions on magnetic resonance imaging. Arthritis Rheum 2007;56:2986-92.

(5) Garnero P, Aronstein WS, Cohen SB, Conaghan PG, Cline GA, Christiansen C, et al. Relationships between biochemical markers of bone and cartilage degradation with radiological progression in patients with knee osteoarthritis receiving risedronate: the Knee Osteoarthritis Structural Arthritis randomized clinical trial. Osteoarthritis Cartilage 2008;16:660-6. Epub 2007 Nov 13.

(6) Manicourt DH, Altman RD, Williams JM, Devogelaer JP, Druetz-Van Egeren A, Lenz ME, et al. Treatment with calcitonin suppresses the responses of bone, cartilage, and synovium in the early stages of canine experimental osteoarthritis and significantly reduces the severity of the cartilage lesions. Arthritis Rheum 1999;42:1159-67.

(7) Ito M, Ikeda K, Nishiguchi M, Shindo H, Uetani M, Hosoi T et al. Multi-detector row CT imaging of vertebral microstructure for evaluation of fracture risk. J Bone Miner Res 2005;20:1828-36.

(8) Graeff C, Timm W, Nickelsen TN, Farrerons J, Marin F, Barker C et al. Monitoring teriparatide-associated changes in vertebral microstructure by high-resolution CT in vivo: results from the EUROFORS study. J Bone Miner Res 2007;22: 1426-33.

(9) Tönnis D. Normal values of the hip joint for the evaluation of X-rays in children and adults. Clin Orthop Relat Res 1976;119:39-47.

(10) Wiberg G. Studies on dysplastic acetabula and congenital subluxation of the hip joint. With special reference to the complication of osteoarthritis. Acta Chir Scand 1939;58: 28-38.

(11) Sharp IK. Acetabular dysplasia: the acetabular angle. J Bone Joint Surg Br 1961;43: 268-272.

(12) Odgaard A, Gundersen HJ. Quantification of connectivity in cancellous bone, with special

emphasis on 3-D reconstructions. Bone 1993; 14:173-182.

(13) Hildebrand T, Rüegsegger P. Quantification of Bone Microarchitecture with the Structure Model Index. Comput Methods Biomech Biomed Engin 1997;1:15-23.

(14) Hahn M, Vogel M, Pompesius-Kempa M, Delling G. Trabecular bone pattern factor - a new parameter for simple quantification of bone microarchitecture. Bone. 1992;13:327-30.

(15) Harrigan TP, Mann RW. Characterization of microstructural anisotropy in orthotropic materials using a second rank tensor. J Mater Sci 1984;19:761-767.

(16) Bauer JS, Link TM, Burghardt A, Henning TD, Mueller D, Majumdar S. et al. Analysis of trabecular bone structure with multidetector spiral computed tomography in a simulated soft-tissue environment. Calcif Tissue Int 2007;80:366-73.

(17) Diederichs G, Link T, Marie K, Huber M, Rogalla P, Burghardt A, et al. Feasibility of measuring trabecular bone structure of the proximal femur using 64-slice multidetector computed tomography in a clinical setting. Calcif Tissue Int 2008;83:332-41.

(18) Ding M, Odgaard A, Hvid I. Changes in the three-dimensional microstructure of human tibial cancellous bone in early osteoarthritis. J Bone Joint Surg Br 2003;85:906-12.
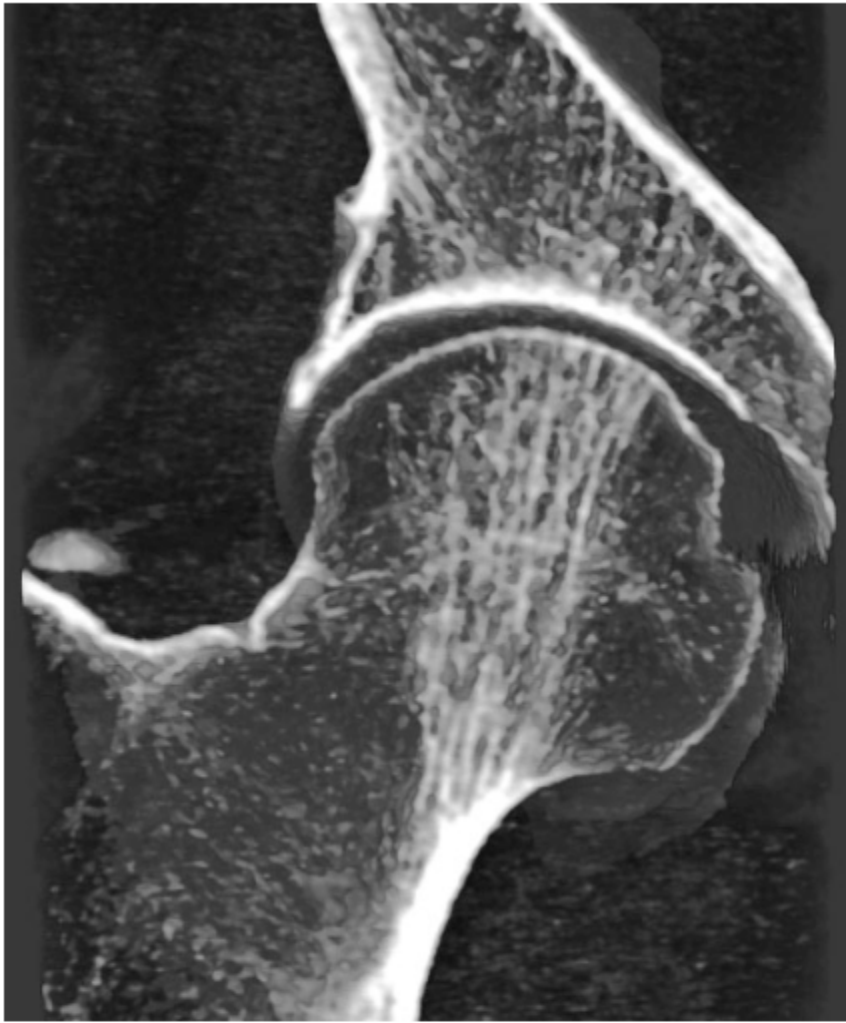
Fig. 1 3D reconstructed MDCT image of a normal hip joint. The principal compressive trabeculae of the femoral head and corresponding acetabular trabeculae are well demonstrated, although the others are not clear because of insufficient spatial resolution.
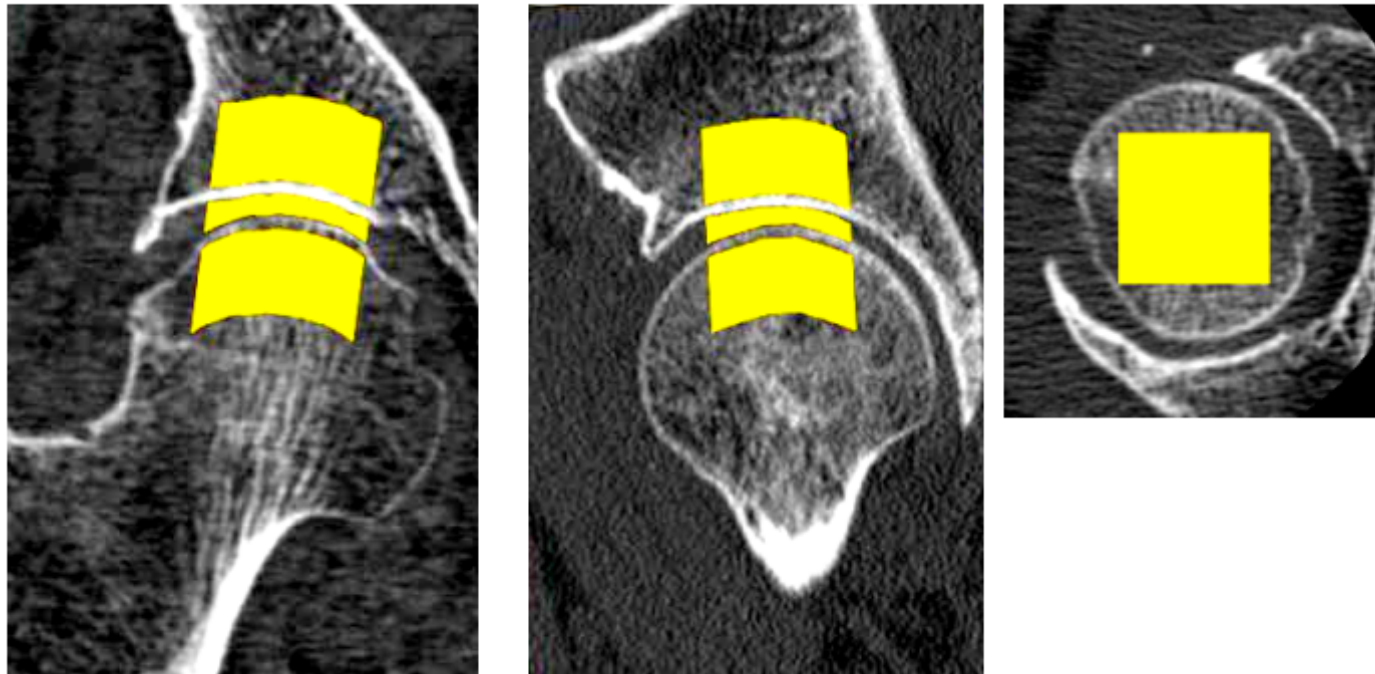
Fig. 2 ROI for the bone microstructure analysis. The subchondral trabecular bone structure of the acetabulum and femoral head and the joint space volume were measured. The subchondral bone region is a 1 cm under the subchondral endplate, 2×2 cm^2 area, and aligned with the principal compressive trabeculae.
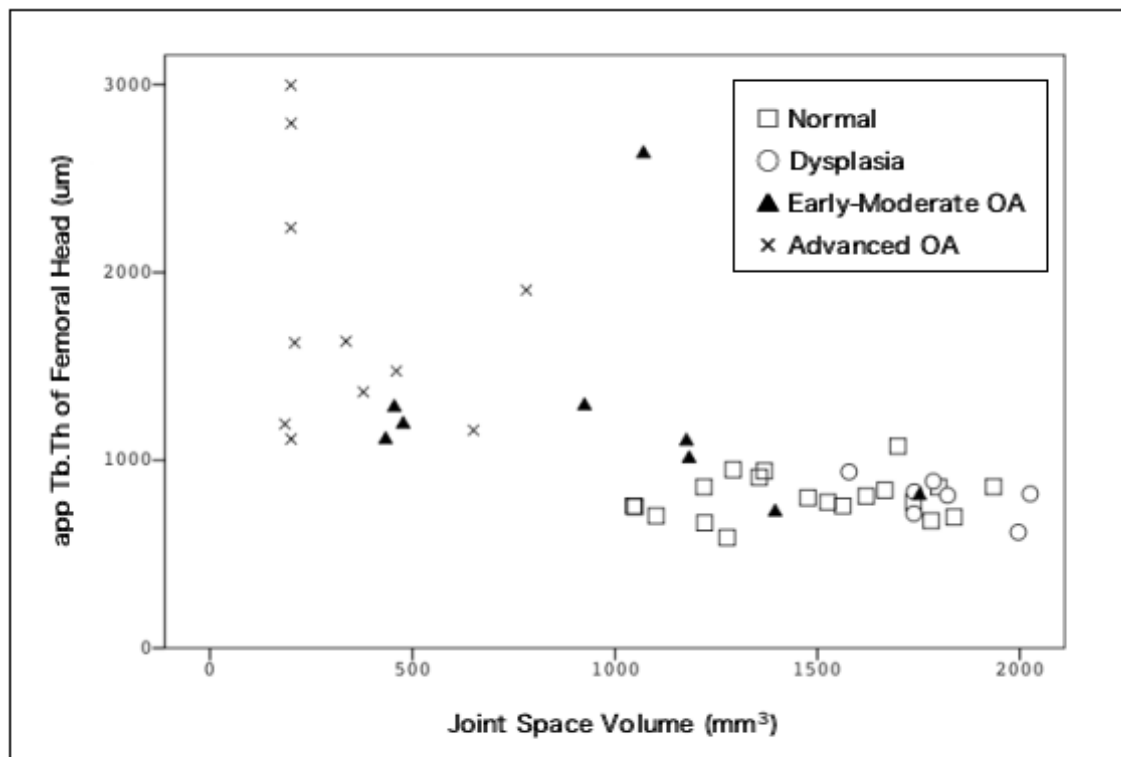
Fig. 3 Relationship between joint space volume and app Tb.Th of femoral head subchondral bone. There is a negative correlation between joint space volume and app Tb.Th. (r=-0.665, p<0.001) App Tb.Th increases in early and advanced staged OA but not in dysplasia.
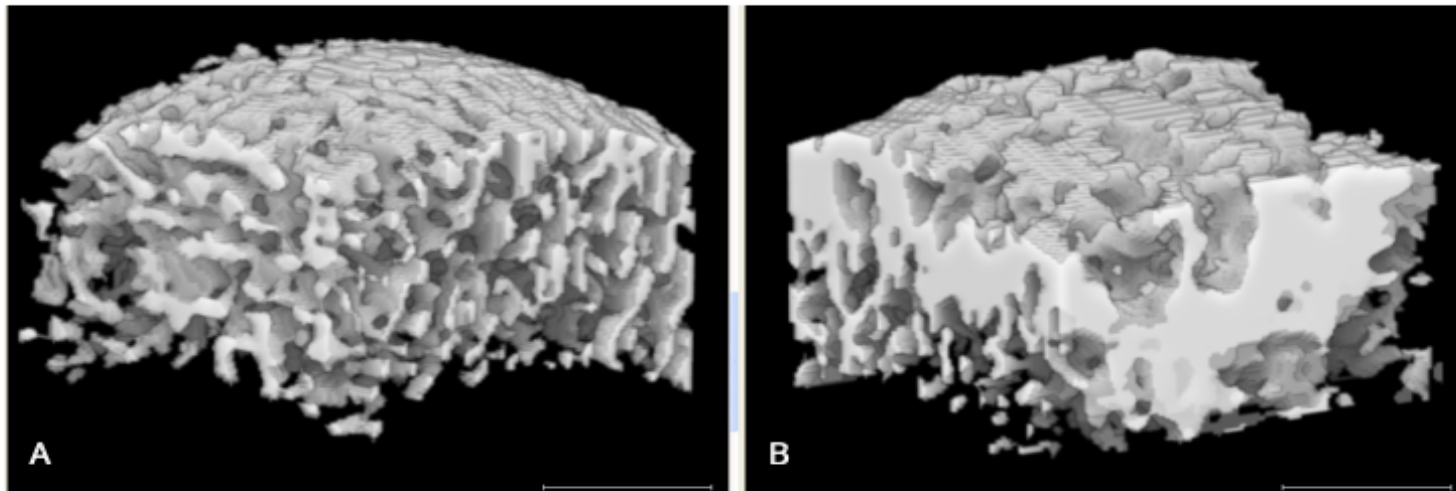
Fig. 4 3D reconstructed MDCT images of femoral head subchondral trabecular bone of a normal subject (A) and an advanced OA patient (B). The subchondral trabecular bone of the OA patient shows mass formation by thick trabecular bones.

Table.1 Relationship between joint space volume and subchondral bone microstructure

	Joint Space Volume vs. Acetabular Bone Structure		Joint Space Volume vs. Femoral Head Bone Structure	
	r	p	r	p
app BV/TV	-0.691	<0.001	-0.729	<0.001
app Tb.Th	-0.628	<0.001	-0.665	<0.001
app Tb.N	0.205	ns	0.435	<0.01
app Tb.Sp	0.41	<0.01	0.192	ns
SMI	0.651	<0.001	0.558	<0.001
TBPf	0.726	<0.001	0.666	<0.001
Euler's N	-0.187	ns	-0.369	<0.05
DA	0.468	<0.001	-0.076	ns

app BV/TV: apparent bone volume fraction, app Tb.Th: apparent trabecular thickness,
app Tb.N: apparent trabecular number, app Tb.Sp: apparent trabecular separation,
SMI: structure model index, TBPf: trabecular bone pattern factor, DA: degree of anisotrophy

Table.2 Relationship between acetabular dysplasia and subchondral bone microstructure

	CE angle vs. Acetabular Bone Structure		CE angle vs. Femoral Head Bone Structure		Acetabuler angle vs. Acetabular Bone Structure		Acetabuler angle vs. Femoral Head Bone Structure	
	r	p	r	p	r	p	r	p
app BV/TV	-0.617	<0.001	-0.429	<0.01	0.393	<0.01	0.257	ns
app Tb.Th	-0.554	<0.001	-0.369	<0.05	0.280	ns	0.139	ns
app Tb.N	-0.115	ns	0.221	ns	0.154	ns	-0.152	ns
app Tb.Sp	0.328	<0.05	0.089	ns	-0.149	ns	-0.136	ns
SMI	0.294	<0.05	0.291	<0.05	-0.382	<0.01	-0.230	ns
TBPf	0.530	<0.001	0.404	<0.01	-0.392	<0.01	-0.286	ns
Euler's N	-0.142	ns	-0.165	ns	-0.055	ns	0.125	ns
DA	0.207	ns	-0.509	<0.001	-0.196	ns	0.272	ns

Table 3 Acetabular subchondral bone microstructure of each group (Mean, 95% CI)

	Normal	Dysplasia	Early-Moderate OA	Advanced OA
app BV/TV (%)	29.8 (26.1, 33.5)	31.8 (23.6, 39.9)	59.1[***][†††] (45.2, 72.9)	73.1[***][†††] (62.0, 84.2)
app Tb.Th (um)	1018 (930, 1106)	1143 (1011, 1276)	1520[**] (1212, 1829)	1909[***][†††] (1563, 2255)
app Tb.N (1/mm)	0.14 (0.13, 0.16)	0.14 (0.11, 0.17)	0.15 (0.13, 0.17)	0.13 (0.11, 0.15)
app Tb.Sp (um)	1111 (1037, 1185)	1259 (953, 1565)	839[†] (590, 1089)	887[†] (657, 1118)
SMI	2.31 (2.16, 2.46)	2.29 (1.74, 2.84)	1.77 (1.13, 2.40)	0.89[***][†††][§] (0.28, 1.51)
TBPf (1/mm)	1.11 (0.90, 1.31)	0.97 (0.46, 1.48)	-0.09[***][††] (-0.52, 0.34)	-0.72[***][†††] (-1.14, -0.30)
Euler's N	-100 (-131, -69)	-76 (-165, 13)	-81 (-126, -35)	-57 (-104, -11)
DA	2.42 (2.13, 2.72)	2.52 (1.26, 3.79)	1.78 (1.51, 2.05)	1.63[*] (1.50, 1.77)

[*] vs. Normal $p<0.05$ [**] vs. Normal $p<0.01$ [***] vs. Normal $p<0.001$
[†] vs. Dysplasia $p<0.05$ [††] vs. Dysplasia $p<0.01$ [†††] vs. Dysplasia $p<0.001$
[§] vs. Early-Moderate OA $p<0.05$

Table 4 Femoral head subchondral bone microstructure of each group (Mean, 95% CI)

	Normal		Dysplasia		Early-Moderate OA		Advanced OA	
app BV/TV (%)	30.2	(24.4, 35.9)	28.5	(17.5, 39.4)	45.6	(30.1, 61.0)	68.5***†††§§	(59.2, 77.9)
app Tb.Th (um)	803	(749, 856)	804	(704, 903)	1240	(811, 1668)	1773***†††§	(1336, 2209)
app Tb.N (1/mm)	0.21	(0.19, 0.24)	0.21	(0.15, 0.27)	0.18	(0.14, 0.23)	0.13**†	(0.10, 0.16)
app Tb.Sp (um)	830	(752, 908)	888	(629, 1146)	803	(645, 961)	746	(586, 906)
SMI	2.03	(1.68, 2.37)	2.09	(1.50, 2.68)	1.59	(0.69, 2.49)	0.66**†	(-0.17, 1.49)
TBPf (1/mm)	1.08	(0.71, 1.45)	1.13	(0.39, 1.88)	0.29	(-0.41, 1.00)	-0.59**†††	(-0.94, -0.23)
Euler's N	-270	(-359, -181)	-247	(-418, -76)	-187	(-306, -68)	-89*	(-139, -39)
DA	1.32	(1.23, 1.42)	1.59*	(1.42, 1.75)	1.57*	(1.37, 1.77)	1.51	(1.40, 1.62)

* vs. Normal $p<0.05$ ** vs. Normal $p<0.01$ *** vs. Normal $p<0.001$
† vs. Dysplasia $p<0.05$ †† vs. Dysplasia $p<0.01$ ††† vs. Dysplasia $p<0.001$
§ vs. Early-Moderate OA $p<0.05$ §§ vs. Early-Moderate OA $p<0.01$